

# Loss-improved electroacoustical modeling of small Helmholtz resonators

Tomasz Starecki<sup>a)</sup>

*Institute of Electronic Systems, Warsaw University of Technology, Nowowiejska 15/19, 00-665 Warsaw, Poland*

(Received 19 September 2006; revised 21 July 2007; accepted 25 July 2007)

Modeling of small Helmholtz resonators based on electroacoustical analogies often results in significant disagreement with measurements, as existing models do not take into account some losses that are observed in practical implementations of such acoustical circuits, e.g., in photoacoustic Helmholtz cells. The paper presents a method which introduces loss corrections to the transmission line model, resulting in substantial improvement of simulations. Values of the loss corrections obtained from comparison of frequency responses of practically implemented resonators with computer simulations are presented in tabular and graphical form. A simple analytical function that can be used for interpolation or extrapolation of the loss corrections for other dimensions of the Helmholtz resonators is also given. Verification of such a modeling method against an open two-cavity Helmholtz structure shows very good agreement between measurements and simulations. © 2007 Acoustical Society of America. [DOI: 10.1121/1.2773929]

PACS number(s): 43.58.Wc, 43.20.Wd, 43.30.Zk, 43.38.Zp [AJZ]

Pages: 2118–2123

## I. INTRODUCTION

Helmholtz resonator is a structure that has found numerous applications. One of them is photoacoustics. Photoacoustic phenomenon relies on producing a thermal and pressure wave due to absorption of light by a substance illuminated by the light.<sup>1</sup> If the light intensity is modulated with an acoustic frequency, absorption of the light results in corresponding, periodic changes of pressure, which means that a sound is generated. Amplitude  $A_{PAS}$  of the sound can be described as<sup>2</sup>

$$A_{PAS} \propto \frac{\alpha P}{fV}, \quad (1)$$

where  $\alpha$  is the light absorption coefficient,  $P$  is the light power,  $f$  the light intensity modulation frequency, and  $V$  the volume of the cell.

Once the photoacoustic signal is produced, its further behavior is purely acoustical. In particular, if the cell is operated at its acoustic resonance frequency, amplitude of the photoacoustic signal will be amplified by the  $Q$  factor of the cell.<sup>2</sup> That is why the Helmholtz structure is one of the most often used cell designs, especially in the case of photoacoustic investigation of solids.<sup>1–3</sup> Such a cell consists of two cavities connected with a duct. Usually the investigated sample is placed in one of the cavities and illuminated with light, while the other cavity is equipped with a sound detector (Fig. 1). One of the main advantages of the Helmholtz resonator applied as a photoacoustic cell is that its overall volume can be kept very small (a few  $\text{cm}^3$  or even below  $1 \text{ cm}^3$ ), which is quite important, as the photoacoustic signal amplitude increases against cell volume (Eq. (1)). Taking into consideration that properties of the cell directly affect sensitivity of

the whole photoacoustic setup, design of the cell should be always given special attention. A common tool used during this process is simulations of the frequency responses of the cells, so that it is possible to evaluate and compare properties of many different cells without having them manufactured, which speeds up the design process and lowers its cost. In the case of photoacoustic Helmholtz cells the most common simulation method is based on acoustoelectrical analogies.

## II. ACOUSTOELECTRICAL ANALOGIES IN MODELING OF PHOTOACOUSTIC HELMHOLTZ RESONATORS

The acoustoelectrical analogies is a well-known method based on the fact that behavior of acoustical elements can be described by means of corresponding electrical components. The photoacoustic Helmholtz resonator from Fig. 1 can be then simulated in a circuit shown in Fig. 2(a), in which cavities are modeled by capacitors, and interconnecting duct by an inductor connected in series with a resistor. The first drawback of the mentioned lumped components model is that there are several sets of definitions that can be used for obtaining  $L$  and  $R$  components values, given, for instance, in the works of Morse,<sup>4</sup> Nolle,<sup>5</sup> Nordhaus and Pelzl.<sup>6,7</sup> But the most important is that no matter which of the mentioned definition sets is used, the model does not produce results that would be in good agreement with measured frequency responses of the resonators.<sup>8</sup> Although simulated resonance frequencies are usually not far away from the measured values, calculated  $Q$  factors of the resonators, which are crucial in photoacoustic applications, differ sometimes as much as about 1000 times from the measurements (if the components are defined as by Morse<sup>4</sup>), and even the definition set that gives the closest match often produces  $Q$  factor values 20 times greater than the measured ones.<sup>9</sup>

Much better results can be obtained if the interconnecting duct is represented by a transmission line (see Fig. 2(b)), which includes viscous and thermal losses.<sup>9</sup> Although use of

<sup>a)</sup>Electronic mail: tomi@ise.pw.edu.pl

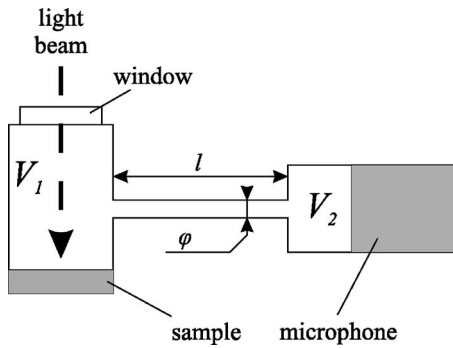


FIG. 1. Sketch of a small Helmholtz resonator applied to photoacoustic investigation of solids.

transmission line model is usually considered when length of the duct is becoming comparable to the acoustical wavelength, the model gives significant improvement also in cases of much shorter ducts, hence it should be used as a standard approach. The transmission line model is based on characteristic impedance  $Z_w$  and propagation constant  $\Gamma_w$  of the line which can be calculated from definitions specified, e.g., in Ref. 10.  $Z_w$  and  $\Gamma_w$  can be then used in conversion of the transmission line into equivalent  $T$  circuit (Fig. 2(c)).<sup>11</sup>

In comparison to the lumped components model, use of the transmission line model results in a much closer prediction of the resonator behavior. However, despite a significant decrease of  $Q$  factor errors, losses are still underestimated, and in some cases the ratio of simulated to measured values of  $Q$  factor still exceeds an order of magnitude (see Table I—column 4).<sup>9</sup>

The transmission line model can be further extended by the introduction of radiation losses  $R_{\text{rad}}$  end corrections  $L_{\text{ends}}$ ,  $R_{\text{ends}}$ ,<sup>5,12–15</sup> acoustical impedance of the microphone  $Z_{\text{micr}}$ ,<sup>16</sup> viscous and thermal losses of the cavities  $R_{vCi}$  and  $R_{tCi}$ ,<sup>5</sup> etc., but the main result of these changes is an increase of complexity of the model (Fig. 3), while its properties are still far away from expectations (see Table I—column 5).<sup>9</sup> Such a

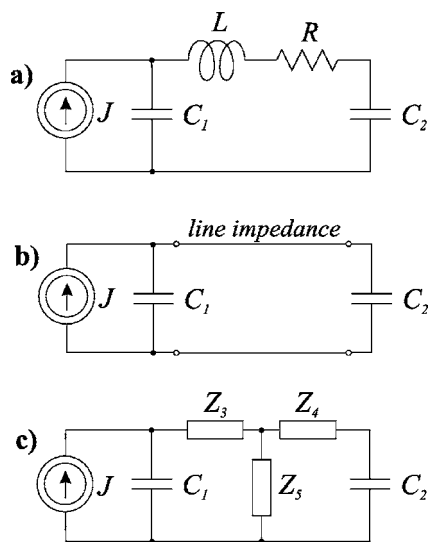


FIG. 2. Models of the resonator presented in Fig. 1, based on acoustoelectrical analogies: (a) lumped components model, (b) transmission line model, (c) transmission line model with the transmission line component replaced by an equivalent lumped  $T$  section.

difference between theoretical and measured properties of the resonators is a bit surprising, taking into consideration that many researchers have investigated properties of Helmholtz resonator and their works show usually much better agreement between theory and measurements (see, for instance, Refs. 17–20). The probable reason is that the mentioned works were conducted on the Helmholtz resonators of much larger size, while at smaller volumes other phenomena become dominant and result in a noticeable increase of the losses inside the resonators.

As a purely theoretical approach was resulting only in different versions of an unsatisfactory model, a practical workaround approach was applied. The goal was to obtain a relatively simple model that would give much closer agreement between theoretical and experimental results.

### III. LOSS CORRECTIONS OF THE TRANSMISSION LINE MODEL

A fact that resonance frequencies obtained from the transmission line model were in good agreement with the measured values, and that the main problem was lack of accuracy regarding simulation of  $Q$  factors, led to the conclusion that not all the losses are included in the model. In small Helmholtz resonators viscous and thermal cavity losses are not the main reason for damping the oscillations. It is more likely that the main sources of losses are flow disturbances (due to rapid change of a cross section at the duct-cavity boundary) and interaction between the jet flowing out of the duct and being reflected by the cavity wall (or the microphone membrane) placed at a relatively small distance in front of the duct opening. Such effects can be modeled by means of resistances  $R_{\text{loss}}$  placed between the components that correspond to acoustical properties of the duct and the cavities (Fig. 4). The resistances  $R_{\text{loss}}$  can be then treated as loss corrections (similarly to the well known end corrections), which include all the losses that occur at the duct-cavity boundaries, including radiation losses, resistive components of end corrections, jet reflection losses, etc. Certainly, in order to obtain noticeable influence of the loss corrections on the frequency responses of the resonators, values of  $R_{\text{loss}}$  must not be much smaller than the real parts of the impedances  $Z_3$  and  $Z_4$ . Hence, it may be convenient to express  $R_{\text{loss}}$  as a function of the impedances  $Z_3$  and  $Z_4$ . In order to simplify the model it was assumed that relationship between  $R_{\text{loss}}$  and  $Z_3, Z_4$  for a given resonator is fixed, so that

$$R_{\text{loss}} = \gamma \text{Re}(Z_3) = \gamma \text{Re}(Z_4). \quad (2)$$

Such an approach is a modified concept of correction factors presented briefly in Ref. 21, where one can also find a detailed description of how to calculate values of the components used in the models presented in Figs. 2 and 3 and of a routine used for extraction of the correction factors. In order to evaluate coefficients  $\gamma$  (retrieved similarly to the mentioned correction factors), frequency responses of 48 different combinations of resonator dimensions were measured and compared to simulated responses. The resonators had 2.0 cm<sup>3</sup> sample cavity, the microphone cavity was 0.5, 1.0, 1.5, and 2.0 cm<sup>3</sup>, and the duct between the cavities was 2.0,

TABLE I. Values of the coefficients  $\gamma$  vs resonator dimensions extracted from the measurements of 48 different Helmholtz resonators and theoretical to measured ratio of  $Q$  factors of these resonators (theoretical  $Q$  factor values calculated from the models given in Figs. 2(c) and Fig. 3).

Duct diameter [mm]	Duct length [cm]	Microphone cavity volume [cm <sup>3</sup> ]	$Q_{\text{theor}}/Q_{\text{meas}}$ (Fig. 2(c))	$Q_{\text{theor}}/Q_{\text{meas}}$ (Fig. 3)	$\gamma$
1	2	0.5	2.00	1.95	0.30
1	2	1	1.49	1.48	0.23
1	2	1.5	1.32	1.31	0.16
1	2	2	1.17	1.16	0.15
1	3	0.5	2.03	1.96	0.22
1	3	1	1.50	1.48	0.15
1	3	1.5	1.39	1.38	0.25
1	3	2	1.23	1.22	0.10
1	4	0.5	2.14	2.07	0.25
1	4	1	1.69	1.66	0.13
1	4	1.5	1.42	1.40	0.15
1	4	2	1.10	1.09	0.10
2	2	0.5	4.08	4.02	0.74
2	2	1	2.33	2.31	0.37
2	2	1.5	1.94	1.92	0.30
2	2	2	1.66	1.65	0.22
2	3	0.5	3.36	3.27	0.61
2	3	1	2.42	2.39	0.35
2	3	1.5	2.00	1.99	0.36
2	3	2	1.69	1.68	0.21
2	4	0.5	3.30	3.23	0.58
2	4	1	2.40	2.37	0.33
2	4	1.5	2.03	2.01	0.28
2	4	2	1.70	1.69	0.20
3	2	0.5	7.56	7.42	1.40
3	2	1	3.67	3.64	0.63
3	2	1.5	2.81	2.79	0.46
3	2	2	2.18	2.17	0.33
3	3	0.5	5.18	5.06	1.13
3	3	1	3.48	3.45	0.59
3	3	1.5	2.70	2.69	0.48
3	3	2	2.13	2.13	0.34
3	4	0.5	5.04	4.97	1.03
3	4	1	3.51	3.47	0.55
3	4	1.5	2.64	2.63	0.42
3	4	2	2.16	2.15	0.34
4	2	0.5	13.17	12.91	2.00
4	2	1	5.67	5.62	0.94
4	2	1.5	3.98	3.96	0.62
4	2	2	2.92	2.91	0.42
4	3	0.5	8.12	7.96	1.70
4	3	1	4.96	4.91	0.92
4	3	1.5	3.66	3.63	0.69
4	3	2	2.84	2.83	0.47
4	4	0.5	7.24	7.11	1.49
4	4	1	4.97	4.92	0.84
4	4	1.5	3.62	3.59	0.63
4	4	2	2.74	2.73	0.49

3.0 or 4.0 cm long and 1.0, 2.0, 3.0 or 4.0 mm in diameter. The obtained values of coefficients  $\gamma$  are presented in Table I and in Fig. 5.

When analyzing the above set of the coefficients  $\gamma$ , it can be easily noticed that they increase with the interconnecting duct diameter and against microphone cavity vol-

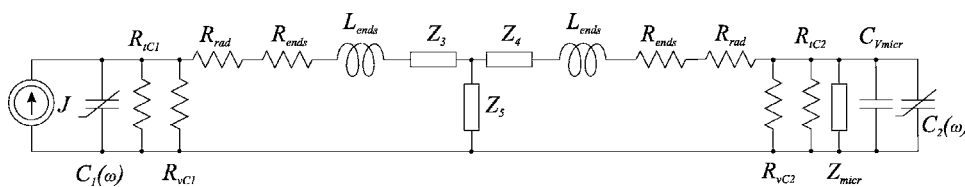


FIG. 3. Enhanced transmission line model including additional loss mechanisms, e.g., radiation impedance, end corrections, microphone impedance, etc.

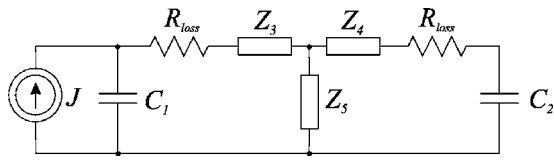


FIG. 4. Simple transmission line model with loss corrections ( $R_{\text{loss}}$ ).

ume, while they are not much influenced by the duct length. This confirms the previous assumption that the transmission line model quite precisely describes losses inside the duct, and that the main loss sources which were not included in the previous models are located outside the duct.

Although a set of coefficients  $\gamma$  is already of some help in the process of designing, having an analytical function describing such coefficients would be much more convenient, especially if applied for modeling purposes. Hence, some further work concentrated on development of such an analytical description. Taking into consideration, that values from Table I show a slightly nonlinear relationship of  $\gamma$  versus duct diameter  $\varphi$ , parabolic approximation was used, so that

$$\gamma = A\varphi + B\varphi^2. \quad (3)$$

In order to find description for  $A$  and  $B$  the following routine was applied. At first all 12 point sets from Fig. 5 were approximated by individual parabolic functions (Fig. 6(a)). The functions were then analyzed in order to obtain a common form as in the Eq. (3) with some efforts made towards compromise between a relatively simple definition of  $A$  and  $B$  and possibly close fit to the given experimental data from Table I, which finally resulted in

$$A = 0.0001 \cdot (1 - 8\ell) \frac{V_1 + V_2}{V_1 V_2}, \quad (4)$$

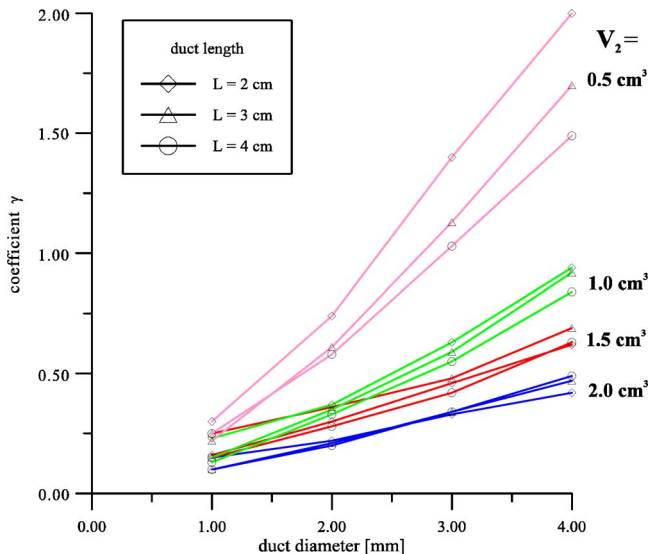


FIG. 5. (Color online) Coefficients  $\gamma$  obtained from measurements of 48 different photoacoustic Helmholtz resonators.

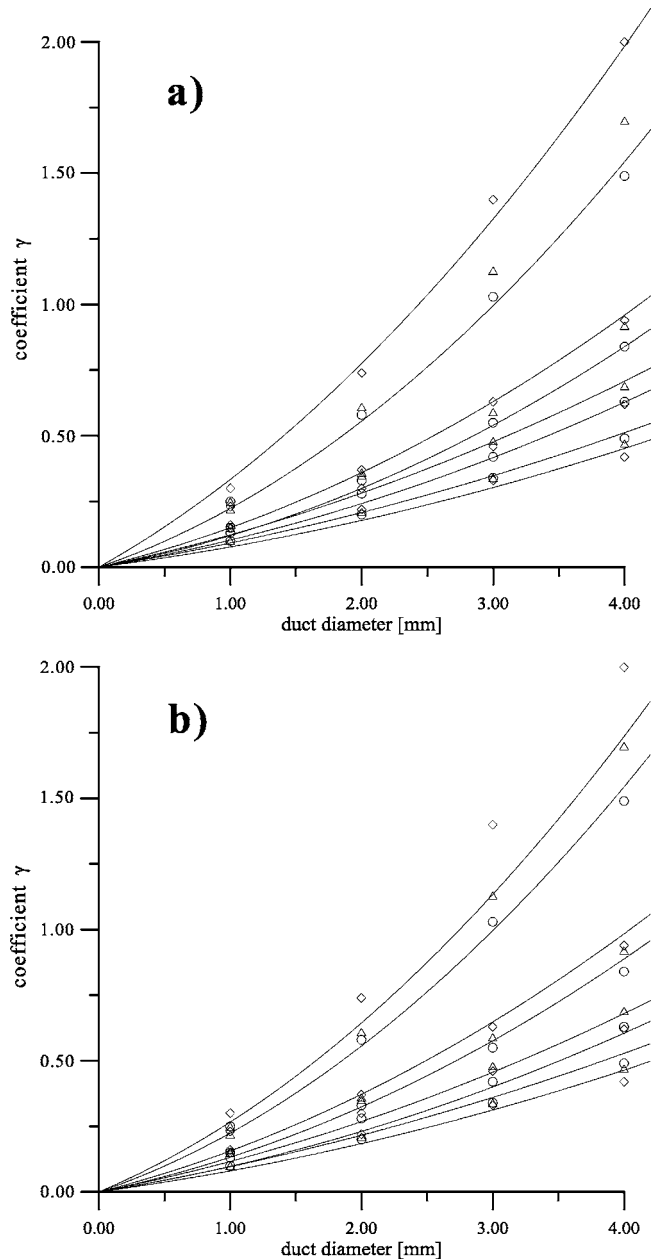


FIG. 6. Approximation of coefficients  $\gamma$  presented in Fig. 5 by analytical functions: (a) with every point set approximated by an individual function, (b) with a single function used for approximation of all the points.

$$B = \sum_{i=1}^2 96,000 \cdot 2^{-2,000,000V_i}, \quad (5)$$

where Eq. (4) is valid only for duct shorter than 12.5 cm (for greater  $\ell$  values,  $A$  should be substituted by zero). In the above equations (Eqs. (2)–(5)) standard SI units should be used (the length and diameter of the duct  $\ell$  should be given in meters, volumes  $V_1$ , and  $V_2$  at both ends of the duct in  $\text{m}^3$ ). In comparison to individual parabolic functions from Fig. 6(a) the above definitions give a little bit worse fit to the experimental data (Fig. 6(b)), but the main character of the relationship is preserved.

The presented loss-improved transmission line components were verified against an open photoacoustic Helmholtz cell. Structure of the cell is shown in Fig. 7(a). In order to

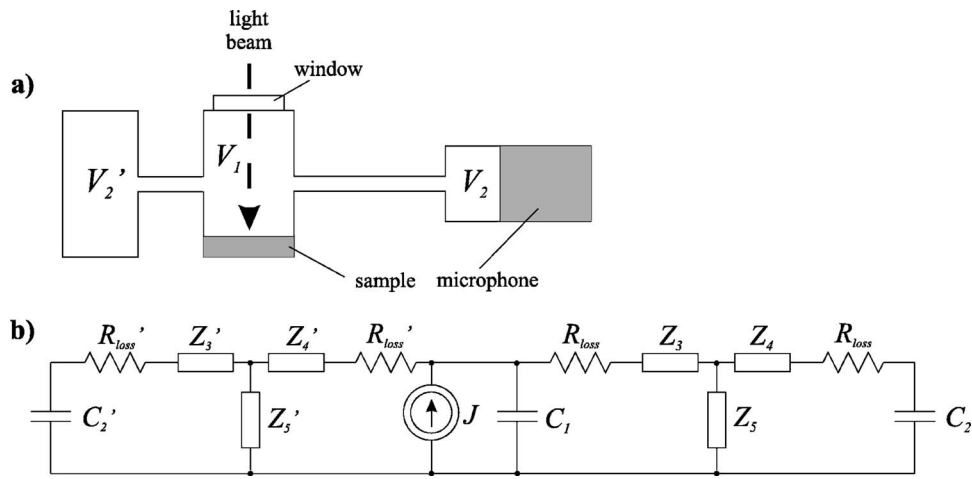


FIG. 7. Triple-cavity Helmholtz resonator (a) and its transmission line model with loss corrections (b) used for simulation of an open dual-cavity Helmholtz resonator (for this purpose volume  $V_2'$  was assigned value of several  $\text{m}^3$ ).

use a similar approach as in dual cavity closed resonator, the external space was treated as an additional cavity  $V_2'$  of a large volume (e.g., a few  $\text{m}^3$ ). Such a resonator can be modeled in a circuit given in Fig. 7(b). In the measured resonator the sample cavity was  $2.0 \text{ cm}^3$  in volume, microphone cavity was  $1.5 \text{ cm}^3$ , duct between the two was  $3.0 \text{ cm}$  in length and  $3.0 \text{ mm}$  in diameter, while the connection between the sample cavity and external space had a form of two parallel ducts:  $5.0 \text{ cm}$  in length and  $2.0 \text{ mm}$  in diameter each. Figure 8 presents measured frequency response of the resonator (black dots) compared with results calculated from the transmission line model without corrections (solid line) and with loss corrections (based on Eqs. (2)–(5); dashed line). The frequency response has two resonance peaks. The one at the higher frequencies results mainly from interaction of the two smaller cavities and the interconnecting duct (that were of

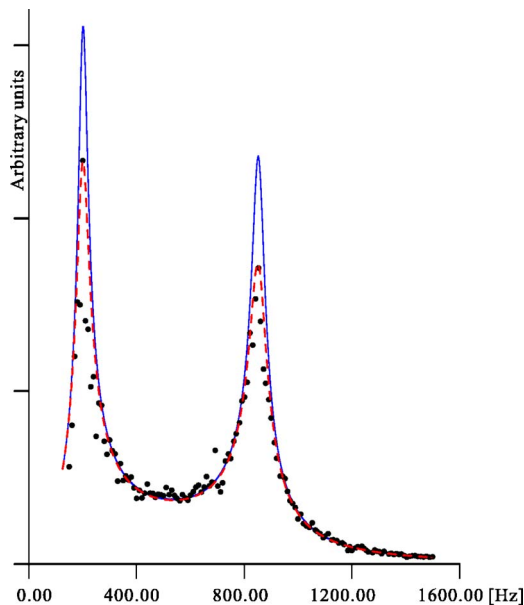


FIG. 8. (Color online) Comparison of measurements of the open two-cavity Helmholtz resonator (black dots) with simulations based on standard transmission line model (solid line) and transmission line model with loss corrections (dashed line).

dimensions identical to one of the resonators measured and used for the purpose of evaluation of the gamma coefficients). The other resonance peak results mainly from the interaction of the third (large) cavity that was connected with the sample cavity with the ducts that were longer than these used for the purpose of evaluation of the gamma coefficients. Good agreement between the simulations and measurements proves that the analytical function describing the gamma coefficients was implemented correctly, because the model works well in the case when partial geometry of the resonator is similar to one of these from which the gamma coefficients were derived (the right resonance peak). It shows that the model also gives very good results in the case when it was used with extrapolation of the loss corrections, when the geometry was different from the previously measured structures (the left resonance peak). It is clearly visible, that although both models (without and with loss corrections) properly reflect actual resonance frequencies, amplitudes measured at the frequencies close to resonances are in good agreement only with the model including loss corrections. Fitting quality of both models was compared by calculation of mean absolute percentage error and root averaged squared error. For the experimental data as given in Fig. 8 the mentioned errors were at the level of 10% and 14% for the best fit of the loss-improved model, while for the best fit of the model without loss corrections the errors were significantly higher (respectively 19% and over 60%), which proves much higher fitting quality of the loss-improved model.

Finally, it should be noticed, that if none of the cavities is small, the values of  $A$  and  $B$  are negligible and the proposed loss-improved model approaches the standard transmission line model from Fig. 2(c). This means that the presented model can be treated as an enhancement which preserves features of the standard transmission line model for the Helmholtz resonators of standard (not very small) size, but which substantially improves modeling results for the resonators of reduced size. The proposed loss-correction model was intended for modeling of Helmholtz resonators

(including multi-cavity structures) with cavities of at least  $0.5 \text{ cm}^3$  and ducts with diameter of 1–4 mm, not shorter than 2 cm.

#### IV. CONCLUSIONS

Some cited works and presented comparison of the measured and simulated frequency responses of a small Helmholtz resonator showed that the standard transmission line model (even with some enhancements like radiation impedance, microphone impedance, end corrections, etc.) based on acoustoelectrical analogies does not produce satisfactory results due to underestimation of losses that occur in the resonator. Proposed improvement of the model was based on the concept of additional loss correction components placed at the ends of the transmission line. Loss corrections were obtained experimentally from a reasonable number of two-cavity Helmholtz resonators and approached by an analytical function, that can be used for interpolation and extrapolation of the correction factors for resonators of some other dimensions. Verification of the presented model with loss corrections against an open multi-cavity Helmholtz resonator showed very good agreement between measured and simulated frequency responses, which leads to the conclusion that the presented approach has a good chance of producing promising results not only in the case of simple two-cavity resonators, but also in the case of complex, multi-cavity small acoustic structures.

<sup>1</sup>Y.-H. Pao, *Optoacoustic Spectroscopy and Detection* (Academic, New York), Chap. 8.

<sup>2</sup>A. Miklós, P. Hess, and Z. Bozóki, "Application of acoustic resonators in photoacoustic trace gas analysis and metrology," *Rev. Sci. Instrum.* **72**, 1937–1955 (2001).

<sup>3</sup>V. P. Zahrov and V. S. Letokhov, *Laser Optoacoustic Spectroscopy*, Springer Series in Optical Sciences (Springer, Berlin, 1986), Vol. **37**, Chap. 5.3.

<sup>4</sup>P. M. Morse, *Vibration and Sound* (McGraw–Hill, New York, 1948), pp. 234–235.

<sup>5</sup>A. W. Nolle, "Small-signal impedance of short tubes," *J. Acoust. Soc. Am.* **25**, 32–39 (1953).

<sup>6</sup>O. Nordhaus and J. Pelzl, "Frequency dependence of resonant photoacoustic cells: The extended Helmholtz resonator," *Appl. Phys.* **25**, 221–229 (1981).

<sup>7</sup>J. Pelzl, K. Klein, and O. Nordhaus, "Extended Helmholtz resonator in low-temperature photoacoustic spectroscopy," *Appl. Opt.* **21**, 94–99 (1982).

<sup>8</sup>T. Starecki, "Modeling of photoacoustic Helmholtz by means of acoustic-electrical analogies," *Electronics Telecommunications Quarterly* **39**, 307–312 (1993).

<sup>9</sup>T. Starecki, *Analiza Porównawcza Modeli Komory Helmholtza do Przyrządów Pomiarowych Typu PAS (Comparative Analysis of Photoacoustic Helmholtz Cell Models-in Polish)* (Ph.D. dissertation, Warsaw University of Technology, Warsaw (1994).

<sup>10</sup>A. H. Benade, "On the propagation of sound waves in a cylindrical conduit," *J. Acoust. Soc. Am.* **44**, 616–623 (1968).

<sup>11</sup>F. B. Daniels, "On the propagation of sound waves in a cylindrical conduit," *J. Acoust. Soc. Am.* **22**, 563–564 (1950).

<sup>12</sup>U. Ingard, "On the theory and design of acoustic resonators," *J. Acoust. Soc. Am.* **25**, 1037–1061 (1953).

<sup>13</sup>R. W. Troke, "Tube-cavity resonance," *J. Acoust. Soc. Am.* **44**, 684–688 (1968).

<sup>14</sup>J. B. Mehl, "Greenspan acoustic viscometer: Numerical calculations of fields and duct-end effects," *J. Acoust. Soc. Am.* **106**, 73–82 (1999).

<sup>15</sup>K. A. Gillis, J. B. Mehl, and M. R. Moldover, "Theory of Greenspan viscometer," *J. Acoust. Soc. Am.* **114**, 166–173 (2003).

<sup>16</sup>A. J. Zuckerwar, "Theoretical responses of condenser microphones," *J. Acoust. Soc. Am.* **64**, 1278–1285 (1978).

<sup>17</sup>A. Selamet, P. M. Radavich, N. S. Dickey, and J. M. Novak, "Circular concentric Helmholtz resonators," *J. Acoust. Soc. Am.* **101**, 41–51 (1997).

<sup>18</sup>M. Moloney, "Quality factors and conductances in Helmholtz resonators," *Am. J. Phys.* **72**, 1035–1039 (2004).

<sup>19</sup>T. A. Johansson and M. Kleiner, "Theory and experiments on the coupling of two Helmholtz resonators," *J. Acoust. Soc. Am.* **110**, 1315–1328 (2001).

<sup>20</sup>J. Wu and I. Rudnick, "Measurements of the nonlinear tuning curves of Helmholtz resonators," *J. Acoust. Soc. Am.* **80**, 1419–1422 (1986).

<sup>21</sup>T. Starecki, "Practical improvements of modeling of photoacoustic Helmholtz cells," *Proc. SPIE* **6159**, 653–658 (2006).